

## Superconductivity from a pseudogapped normal state: A mode-coupling approach to precursor superconductivity

Jiri Maly, Boldizsár Jankó, and K. Levin

*The James Franck Institute, The University of Chicago, 5640 S. Ellis Avenue, Chicago, Illinois 60637*

(Received 16 March 1998)

We derive a phase diagram for the pseudogap onset temperature  $T^*$  (associated with the breakdown of the Fermi-liquid state, due to strong pairing correlations) and the superconducting instability  $T_c$  as a function of variable pairing strength  $g$ . Our diagrammatic approach represents a systematic application of the pairing decoupling scheme of Kadanoff and Martin to arbitrary  $g$  and temperatures  $T > T_c$ . This self-consistent, conserving scheme reveals a delicate competition between the growth (with increasing  $g$ ) of the pseudogap magnitude and that of  $T_c$ . [S0163-1829(99)03802-3]

It is generally agreed that the pseudogap state of the underdoped cuprates represents some type of pairing above  $T_c$  which is postulated to derive from neutral spinon pairs,<sup>1</sup> spin density wave states,<sup>2</sup> or from some form of  $(2e)$  Cooper pairing which foreshadows the ultimate superconducting state. Each of these scenarios must not only address the nature of the exotic (i.e., pseudogapped) normal state but also the transition from this state to its associated superconducting instability. In this paper we investigate these issues under the presumption that the normal state spectral function gap is associated with superconducting correlations which set in at temperatures  $T^*$  well above  $T_c$ . Our results are consolidated into a quantitative phase diagram in which the pseudogap phase occupies a large temperature range in the limit of moderately strong superconducting coupling  $g$ . Because of our current emphasis on  $s$ -wave pairing in three dimensions, direct comparison with experiment will be deferred to a future paper.

There has been an extensive literature on the effects of variable  $g$  on  $T_c$  in the context of interpolating between the BCS (small  $g$ , free fermions above  $T_c$ ) and the Bose Einstein (large  $g$ , bound fermions above  $T_c$ ) limits.<sup>3-7</sup> Our contribution is to approach this crossover problem using a diagrammatic formulation which is based on a Green's function decoupling scheme of Kadanoff and Martin.<sup>8</sup> We refer to this as "mode-coupling" theory, since it self-consistently treats the coupling of the single particle and pair propagators. These authors have argued that such a scheme correctly captures the physics of pairing correlations. Here our calculations of  $T_c$  demonstrate that the Bose-Einstein (BE) condensation temperature is approached *from below*, with increasing  $g$ , as is expected physically.<sup>9</sup> Moreover, as the system becomes progressively more two dimensional  $T_c \rightarrow 0$ ,<sup>10</sup> while the chemical potential  $\mu$  is properly positive at small  $g$ . Both of these observations are in contrast to earlier work<sup>4,5</sup> in which self-energy effects were not fully treated. It should be noted that near, but above  $T_c$  our equations assume a particularly simple form in which the single particle Green's function, the Thouless criterion (or  $T_c$  equation) and the number equation coincide with their counterparts obtained in the standard superconducting theory but with the pseudogap playing the role of the superconducting gap.

We have previously<sup>11</sup> studied the Kadanoff and Martin scheme at "lowest order," in which mode-coupling effects are neglected. This approach is suitable for addressing the breakdown of the Fermi liquid at  $T^*$ , and for studies at higher  $T$ . It was demonstrated that this breakdown coincides with the onset of *resonant* structure in the  $T$  matrix.<sup>11</sup> As a result of pair resonances, the single particle lifetime  $\text{Im} \Sigma$  near  $k_F$  acquires a maximum rather than the usual (quadratic Fermi liquid) minimum, as a function of frequency. A physical picture of the pseudogap phase thus emerges: this state consists of long lived (but *not preformed*) pairs which introduce a gap in the electronic spectral function by blocking available single particle states around the Fermi surface. The resonant state is naturally intermediate between the free fermions of weak coupling, and the bound fermions of the strong coupling limits.

Our approach is based on a generic three-dimensional (3D) Hamiltonian consisting of fermions in the presence of an  $s$ -wave attractive interaction,  $V_{\mathbf{k},\mathbf{k}'} = g \varphi_{\mathbf{k}} \varphi_{\mathbf{k}'}$ , where  $\varphi_{\mathbf{k}} = (1 + k^2/k_0^2)^{-1/2}$  and  $g < 0$  is the coupling strength expressed in units of  $g_c = -4\pi/mk_0$ .<sup>12</sup> In the present decoupling scheme the three fundamental coupled equations are obtained by combining the number equation constraint with the self-energy and  $T$ -matrix equations appropriate to the pairing decoupling approximation<sup>13,8,14</sup>

$$\Sigma_{\mathbf{k},i\omega_l} = T \sum_{\mathbf{q},\Omega_m} t_{\mathbf{q},i\Omega_m} G_{\mathbf{q}-\mathbf{k},i\Omega_m-i\omega_l} \varphi_{\mathbf{k}-\mathbf{q}/2}^2, \quad (1)$$

$$t_{\mathbf{q},i\Omega_m}^{-1} = g^{-1} + T \sum_{\mathbf{k},\omega_l} G_{\mathbf{k},i\omega_l} G_{\mathbf{q}-\mathbf{k},i\Omega_m-i\omega_l} \varphi_{\mathbf{k}-\mathbf{q}/2}^2, \quad (2)$$

where the Green's function is given by  $G_{\mathbf{k},i\omega_l}^{-1} = G_{\mathbf{k},i\omega_l}^{(0)-1} - \Sigma_{\mathbf{k},i\omega_l}$ ,  $G_{\mathbf{k},i\omega_l}^{(0)-1} = i\omega_l - \epsilon_{\mathbf{k}}, \Omega_m/\omega_l$  are the even/odd Matsubara frequencies, and the electronic dispersion is  $\epsilon_{\mathbf{k}} = k^2/2m - \mu$ .

These equations must be solved numerically. For temperatures at and above  $T^*$ , the "lowest order" theory is adequate and all Green's functions in Eqs. (1) and (2) may be replaced by bare propagators.<sup>11</sup> The transition from the Fermi-liquid breakdown to the well established pseudogap phase is difficult to treat and its detailed characterization will

be deferred to a future paper. From the well-established pseudogap state, down to  $T_c$ , the numerics again become tractable.

In this paper we address this last regime, beginning directly with  $T_c$ . We use two numerical algorithms which are both based on a convergence scheme associated with a parametrization of the unknown functions of momentum and frequency in Eqs. (1) and (2). This parametrization is justified by numerical studies. A direct numerical attack on the problem using the full equations is difficult to implement as well as assess because of restriction to a finite set of Matsubara frequencies; the present work will lay the necessary ground work for such a future program.

For the purposes of calculating  $T_c$ , the largest contribution to the self energy in Eq. (1), may be seen to come from the low frequency, long wavelength phase space region where the  $T$  matrix is large. As will be justified numerically below, the integral is well approximated by<sup>15</sup>

$$\Sigma_{\mathbf{k},\omega} \approx -\Delta_{\text{pg}}^2 \varphi_{\mathbf{k}}^2 G_{\mathbf{k},-\omega}^{(0)}. \quad (3)$$

It follows from this equation that

$$t_{0,0}^{-1} = g^{-1} + \sum_{\mathbf{k}} \frac{1-2f(E_{\mathbf{k}})}{2E_{\mathbf{k}}} \varphi_{\mathbf{k}}^2, \quad (4)$$

where  $E_{\mathbf{k}} = \sqrt{\epsilon_{\mathbf{k}}^2 + \Delta_{\text{pg}}^2 \varphi_{\mathbf{k}}^2}$ . The pseudogap parameter which appears in Eq. (3) is defined to be

$$\Delta_{\text{pg}}^2 = \sum_{\mathbf{q}} \int_{-\infty}^{\infty} \frac{d\Omega}{\pi} b(\Omega) \text{Im} t_{\mathbf{q},\Omega}, \quad (5)$$

where  $f(\omega), b(\omega) = [\exp(\omega/T) \pm 1]^{-1}$ . It is evident that  $\Delta_{\text{pg}}^2$  in Eq. (5) coincides with the square amplitude of pairing fluctuations  $g^2 \langle c^\dagger c^\dagger c c \rangle$  which can be defined more generally away from  $T_c$ .

In order to evaluate  $T_c$ , Eq. (5) must be combined with the Thouless criterion from Eq. (4), along with the number equation. The three fundamental equations for  $T_c$  are Eq. (5), along with

$$1 + g \sum_{\mathbf{k}} \frac{1-2f(E_{\mathbf{k}})}{2E_{\mathbf{k}}} \varphi_{\mathbf{k}}^2 = 0, \quad (6)$$

$$2 \sum_{\mathbf{k}} \left[ v_{\mathbf{k}}^2 + \frac{\epsilon_{\mathbf{k}}}{E_{\mathbf{k}}} f(E_{\mathbf{k}}) \right] = n, \quad (7)$$

where  $v_{\mathbf{k}}^2 = (1 - \epsilon_{\mathbf{k}}/E_{\mathbf{k}})/2$ .

It should be noted that Eqs. (3), (6), and (7) show that the single particle Green's function, the Thouless criterion and the number equation assume a particularly simple form which coincides with their (below  $T_c$ ) counterparts obtained in the standard superconducting theory but with the pseudogap playing the role of the superconducting gap. This simplicity (as well as the related BCS-like behavior, at small  $g$ , below<sup>8</sup>  $T_c$ ) would not obtain if fully renormalized Green's functions are used everywhere.<sup>9,16,17</sup>

Equations (5)–(7) can be viewed as a simple (one variable,  $\Delta_{\text{pg}}$ ) parametrization of Eqs. (1) and (2). As an important check on our numerical results and on the approximation in Eq. (3), we have implemented an alternative numerical scheme. We study Eqs. (1) and (2) slightly above  $T_c$ , and

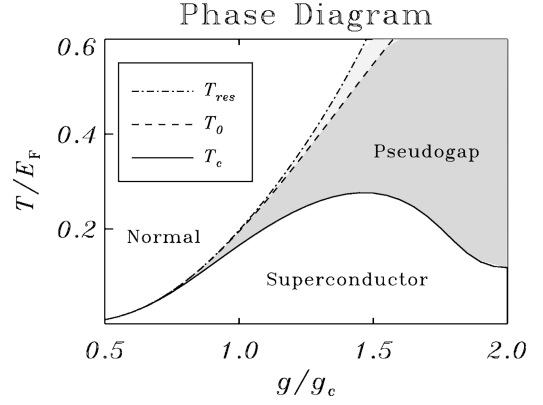


FIG. 1. Pseudogap phase diagram, which indicates the Fermi liquid breakdown corresponding to pair resonance onset, at  $T_{\text{res}} = T^*$ , the fully self-consistent  $T_c$  and the transition temperature  $T_0$  in the absence of mode coupling.

thereby characterize the self-energy and diverging  $T$  matrix. This method is facilitated by introducing a parametrized form for the latter

$$t_{\mathbf{q},\Omega}^{\text{model}} = \frac{g(a'_0)^{-1}}{\Omega - \Omega_{\mathbf{q}} + i\Gamma_{\mathbf{q}}}, \quad (8)$$

as well as an additional variational parameter,  $\gamma$ , in the self-energy of Eq. (3)

$$\Sigma_{\mathbf{k},\omega}^{\text{model}} = -\frac{\Delta_{\text{pg}}^2 \varphi_{\mathbf{k}}^2}{\omega + \epsilon_{\mathbf{k}} + i\gamma}. \quad (9)$$

Equation (8) reflects the analytic form (at low  $\Omega$  and  $\mathbf{q}$ ) of the divergence in the  $T$  matrix in the immediate vicinity of the superconducting instability. It is justified only as an approximation for computing  $\Sigma$ , not as representing the full complex structure of the  $T$  matrix. Here we introduce three parametric variables:  $a'_0$  is a real number of order unity, and the real parameters  $\Omega_{\mathbf{q}}$  and  $\Gamma_{\mathbf{q}}$ .

The coupled equations for  $\Sigma_{\mathbf{k},\omega}$  and  $t_{\mathbf{q},\Omega}^{-1}$ , as a function of temperature, were solved numerically using the model self-energy and  $T$  matrix of Eqs. (9) and (8). In a given iteration  $\Delta_{\text{pg}}, \gamma$  were used to compute  $t_{\mathbf{q},\Omega}$  via Eq. (2) which was then approximated by Eq. (8) for use in Eq. (1). The output of the latter was then used to extract  $\Delta_{\text{pg}}$  and  $\gamma$  via (least squares) fits to Eq. (9) and the procedure repeated until convergence of the parametrization was obtained. In this way, we find that as  $T_c$  is approached the parameter  $\gamma$  in Eq. (9) converges to zero, as is implied by Eq. (3). In addition  $T_c$  can be extracted as the point at which the  $T$  matrix diverges so that  $\Omega_{\mathbf{q}}$ , and  $\Gamma_{\mathbf{q}}$  simultaneously vanish.<sup>18</sup> This value agrees to within about 0.90 with that obtained from Eqs. (5)–(7). It should be stressed that this maximum in  $\text{Im} \Sigma_{\mathbf{k},\omega}$  is a continuation of the (much weaker) peak at  $\omega = -\epsilon_{\mathbf{k}}$  which was found in Ref. 11 as the Fermi liquid breaks down near  $T^*$ . With lower  $T$  this peak grows progressively sharper until the instability at  $T_c$  is reached. [For a typical self-energy curve, near  $T_c$ , see inset to Fig. 3(a) below.]

Our numerical results from Eqs. (5)–(7) are presented first as a phase diagram in Fig. 1. Also shown is the temperature  $T^*$  at which the Fermi liquid first breaks down, as found in Ref. 11. The dotted line indicates the superconducting instability temperature  $T_0$  computed in the absence of mode coupling. When there is an appreciable pseudogap,  $T_c$  and

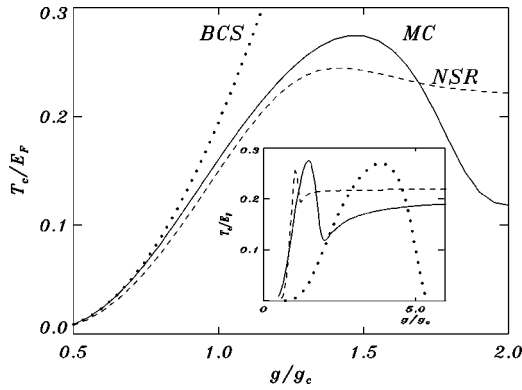


FIG. 2. Comparison of the  $T_c$  curves in BCS theory, the Gaussian approximation of Nozières and Schmitt-Rink (NSR), and our mode coupling theory (MC). The inset plots the variation of  $T_c$  for three different pairing interaction ranges with variable  $k_0/k_F$  ( $=1$ , solid), ( $=4$ , dashed), ( $=1/4$ , dotted).

$T^*$  vary in an inverse fashion with  $g/g_c$ . This is a consequence of the pseudogap which suppresses  $T_c$ , but is not present at  $T^*$ . In this way the pseudogap regime is greatly enhanced by mode-coupling contributions.

The overall behavior of  $T_c$  is compared with that obtained from the approximation of Ref. 4, as well as that of strict BCS theory in Fig. 2. The nonmonotonic behavior of  $T_c$  results from the facts that (1) the high  $g$  asymptote must be approached from below<sup>9</sup> and (2) as in Ref. 4, the low  $g$  exponential dependence tends to overshoot this asymptote. Here, the overshoot is even more marked than in Ref. 4 because of self-energy effects which pin  $E_F$  at  $\mu$ . Point (1) above is a consequence of the decreasing pair size and concomitant reduction of the Pauli principle repulsion. While not shown here, it can be seen, that the maximum in  $T_c$  is associated with  $\mu \sim \Delta_{pg}$  and the minimum with  $\mu = 0$ . Indeed, the complex behavior of  $T_c$  shown in Fig. 2 can be understood on general physical grounds. A local maximum appears in the  $T_c$  curve as a consequence of a growing (with increased coupling) pseudogap  $\Delta_{pg}$  in the fermionic spectrum which weakens the superconductivity. However, even as  $\Delta_{pg}$  grows, superconductivity is generally sustained. In the present scenario, superconductivity is preserved by the conversion of an increasing fraction of fermions to bosonic states, which can then Bose condense. Once the fermionic conversion is complete ( $\mu = 0$ ),  $T_c$  begins to increase again with coupling.

The behavior of  $T_c$  on an expanded coupling constant scale, for different ranges of the interaction (parametrized by  $k_0/k_F$ ) is shown in the inset to Fig. 2. The limiting value of  $T_c$  for large values of  $g/g_c$  approaches the ideal Bose-Einstein condensation temperature  $T_{BE} = 0.218E_F$  as  $k_0 \rightarrow \infty$ . The qualitative shape of the  $T_c$  curve, however, is retained as long as  $k_0/k_F$  is greater than about 0.5.

Results for the behavior away from  $T_c$  obtained by iterative solution of the parametrized form of Eqs. (1) and (2) are represented in Figs. 3(a) and 3(b), as plots of the characteristic parameters for the electronic and pair propagators, respectively. The shaded regions indicate where the  $\Sigma$  parametrization breaks down, and the insets plot the calculated imaginary parts of  $\Sigma$  and the  $T$  matrix, obtained following the iterative prescription discussed earlier. At higher  $T$ , be-

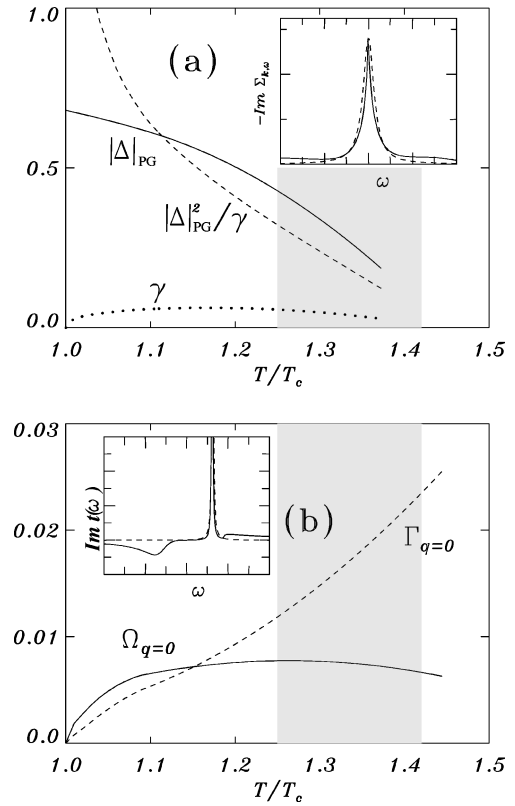


FIG. 3. Evolution of the parameters (in units of  $E_F$ ) which characterize the electronic self-energy (a) of Eq. (9) and  $T$  matrix (b) of Eq. (8). Shaded region represents the breakdown of Eq. (9) as well as lowest order theory. The latter is valid to right of shaded region. The values of  $\Delta_{pg}^2/\gamma$  divided by a factor of 10,  $g/g_c = 1.2$ . Calculated imaginary components of self-energy and  $T$  matrix are plotted in the insets, for general  $T/T_c$  near 1.0, along with their Lorentzian (dashed line) fitted curves, so that at any  $T/T_c$  the units on the figure can be deduced. For example, for (a), Lorentzian width =  $\gamma$ , height =  $\Delta_{pg}^2/\gamma$ .

yond the shaded region, the solutions are given by the lowest order theory. For the pair parameters we extrapolate through this region to join onto the lowest order theory. It can be seen that feedback effects, associated with a pseudogap in the single particle spectrum, lead to a (slightly smeared) gap in the imaginary part of the inverse  $T$  matrix so that when  $\Omega_q < \Delta_{pg}, \Gamma_q$  remains small. This latter parameter reflects, in turn, the small size of the single particle inverse lifetime  $\gamma$ , which by iteration is conveyed back to constrain  $\Gamma_q$ . Thus mode coupling leads to a *stabilization* of resonance effects and, thereby, an amplification of pseudogap behavior. These results lead to the conclusion that, upon heating, the weakening of the pseudogap in the spectral function arises via a reduction in  $\Delta_{pg}$ , while the single particle inverse lifetime ( $\gamma$ ) remains relatively small, at least for some substantial range of  $T$ .

In summary, within a BCS–Bose-Einstein crossover picture, we have presented a *quantitative* phase diagram which compares the temperature onset of the pseudogap with the onset of a superconducting state, associated with pseudogapped fermions. Mode-coupling effects, which were important for this analysis, considerably enhance the pseudogap regime. We have demonstrated (for the  $s$ -wave case) that this pseudogap in the spectral function disappears

with temperature, as it evolves into a Fermi-liquid state, principally by a reduction in the gap size  $\Delta_{pg}$ . While we have not established detailed connections to the cuprates, some aspects about the hole concentration dependence can be noted.<sup>19</sup> Of additional importance for the cuprates is the prediction that the effective inverse lifetime in the electronic self-energy  $\gamma$ , which can be deduced experimentally,<sup>20</sup> varies continuously to zero at  $T_c$ . Finally changes in our results associated with the  $d$ -wave, layered structure of the high- $T_c$  systems can be anticipated: the nodal structure of  $d$ -wave pairs will weaken the gap in the  $T$  matrix which played an important role in determining the detailed temperature evolution of  $\Delta_{pg}(T)$  and  $\gamma(T)$  above  $T_c$ . Moreover, *quasi-two*

*dimensionality will considerably lower the energy scales and enhance the pseudogap regime, particularly as the insulator is approached. Despite these omissions, our physical picture of the interplay of the pseudogap and superconducting instability is expected to be qualitatively general and should apply to the  $d$ -wave, quasi-2D case, as well.*

We would like to thank A. Abanov, Qinjin Chen, M. Norman, Y. Vilk, and, especially I. Kosztin for useful discussions. This research was supported in part by the Natural Sciences and Research Council of Canada (J.M.) and the Science and Technology Center for Superconductivity funded by the National Science Foundation under Grant No. DMR 91-20000.

<sup>1</sup>P. W. Anderson, *The Theory of Superconductivity in the High- $T_c$  Cuprate Superconductors* (Princeton University Press, Princeton, 1997).

<sup>2</sup>A. V. Chubukov, D. Pines, and B. P. Stojkovic, *J. Phys.: Condens. Matter* **8**, 10 017 (1996); J. R. Schrieffer and A. P. Kampf, *J. Phys. Chem. Solids* **56**, 1673 (1995).

<sup>3</sup>A. J. Leggett, *J. Phys. (Paris)* **41**, C7 (1980).

<sup>4</sup>P. Nozières and S. Schmitt-Rink, *J. Low Temp. Phys.* **59**, 195 (1985).

<sup>5</sup>M. Randeria, J. M. Duan, and Ly Shieh, *Phys. Rev. Lett.* **62**, 981 (1989); C. A. R. Sa de Melo, M. Randeria, and J. R. Engelbrecht, *ibid.* **71**, 3202 (1993).

<sup>6</sup>See, for example, R. Micnas, J. Ranninger, and S. Robaszkiewicz, *Rev. Mod. Phys.* **62**, 113 (1990); J. Ranninger and J. M. Robin, *Phys. Rev. B* **53**, R11 961 (1996).

<sup>7</sup>N. Trivedi and M. Randeria, *Phys. Rev. Lett.* **75**, 312 (1995).

<sup>8</sup>L. P. Kadanoff and P. C. Martin, *Phys. Rev.* **124**, 670 (1961); A. Klein, *Nuovo Cimento* **25**, 788 (1962).

<sup>9</sup>R. Haussmann, *Phys. Rev. B* **49**, 12 975 (1994).

<sup>10</sup>We thank Ioan Kosztin and Qinjin Chen for pointing out these 2D results.

<sup>11</sup>B. Janko, J. Maly, and K. Levin, *Phys. Rev. B* **56**, R11 407 (1997).

<sup>12</sup>While we consider the  $s$ -wave symmetry case,  $d$ -wave symmetry can be readily introduced via the  $\varphi_{\mathbf{k}}$ , and in the 2D limit.

<sup>13</sup>B. R. Patton, Ph.D. thesis, Cornell University, 1971.

<sup>14</sup>The detailed form used here for the  $T$  matrix is more readily related to that in Ref. 13 than in Ref. 8. It should also be noted that we have verified that this diagrammatic scheme is consistent with the general criteria for number conservation in G. Baym and L. P. Kadanoff, *Phys. Rev.* **124**, 287 (1961).

<sup>15</sup>Here we have dropped a structureless term which may be parametrized as  $\Sigma_0$ . This is relatively unimportant when the self-energy is integrated over, as in computing  $T_c$ . However, it will contribute to properties such as the density of states where it is necessary to regularize the self-energy so that it is never a strict delta function in the normal state.

<sup>16</sup>O. Tchernyshyov, *Phys. Rev. B* **56**, 3372 (1997).

<sup>17</sup>J. J. Deisz, D. W. Hess, and J. W. Serene, *Phys. Rev. Lett.* **80**, 373 (1998).

<sup>18</sup>It should also be noted that the imaginary part of  $a_0$  vanishes at  $T_c$ . Moreover, in numerical iterations, especially near  $T_c$ , a Landau-Ginzburg (small  $q$ ) expansion was used to simplify various integrals.

<sup>19</sup>Pseudogap effects are expected to increase, as the insulator is approached, as a consequence of a three- to two-dimensional crossover, as well as a reduction in the plasma frequency; see J. Maly, K. Levin, and D. Z. Liu, *Phys. Rev. B* **54**, 15 657 (1996).

<sup>20</sup>M. Norman (unpublished).